300-GHz-Bandwidth Network Analysis Using Time-Domain Electro-Optic Sampling

H. Cheng and J.F. Whitaker
Center for Ultrafast Optical Science

University of Michigan

ABSTRACT

We have demonstrated *S*-parameter measurements on simple passive circuit elements with 300-GHz bandwidth using an external-electro-optic, time-domain sampling technique. Clean, wideband input pulses were generated and transmitted to the device under test in a novel test fixture which integrated the optoelectronic signal source, the coplanar transmission lines, and the element to be measured on a monolithic low-permittivity substrate. A dramatic increase in the fidelity of short-electrical-pulse transmission, as evidenced by a 75% improvement of 3-dB bandwidth after 2 mm of propagation, was observed on a coplanar stripline supported by a quartz substrate when compared with a circuit fabricated on a GaAs substrate having permittivity approximately three times greater. The availability of this enhanced bandwidth has led to the demonstrated network analysis in the submillimeter-wave range using guided signals.

INTRODUCTION

Time-domain device characterization using the laser-based electro-optic and photoconductive sampling techniques has proven to be a valuable tool for directly measuring high-frequency behavior that is impossible to access using traditional network analyzers [1]-[3]. Typical time-domain network analysis is performed by measuring the incident, reflected, and transmitted electrical waveforms on transmission lines at the input and output of a device under test. From these waveforms, time-domain information can be converted to the frequency domain through numerical Fast-Fourier-Transform routines, and the *S*-parameters of the device can be calculated. There are two constraints, however, in the design and realization of this transmission-line "test fixture" required for the time-domain characterization. First, the pulse generation site (in optically-based systems, usually a photoconductive switch) must be located several millimeters away from the device under test in order to separate the real measured signal from any reflections arising from the imperfect loads present in this high-bandwidth system. Secondly, the position where the waveforms are actually probed must be typically 0.5 mm to 1 mm from the device under test in order to distinguish between the incident and reflected waveforms that can become superimposed for actual measurement planes closer to the device. Although the bandwidths of both the pulse-generation and the waveform-measurement techniques are in the terahertz regime, attenuation and dispersion within the transmission-line test fixture will arise from the air-substrate permittivity discontinuity. This has imposed a severe limitation on the bandwidth of time-domain characterization techniques, so that successful measurements have generally reached only to ~ 100 GHz. [1,2]

One alternative to eliminating the permittivity mismatch present in these structures would be to add a superstrate having a similar dielectric constant as the substrate. However, this approach is not practical for substrates already supporting devices, since their surface topology is not flat, and there must not be any air gap remaining between the dielectric cap and the substrate if the field is to be totally confined. Another approach is to remove the substrate from under the coplanar transmission lines so that they would be left suspended in air. However this approach lacks the necessary rigid support supplied by a substrate for a traditional semiconductor device. The solution followed in this work to alleviate these problems has been to produce a high-bandwidth coplanar-strip (CPS) transmission line residing on a low-permittivity, non-semiconducting substrate, but which is also integrated with a fast photoconductive generator. This structure has been employed as a robust, high-bandwidth test fixture for use in two-port, submillimeter-wave network analysis.

The crucial integration of a high-bandwith test signal source with low-distortion transmission lines and a device under test was accomplished through a process known as epitaxial lift-off. [4] A thin film of ultrafast-response low-temperature-grown GaAs (LT-GaAs)[5] was removed from its native substrate, grafted onto a low-permittivity fused silica or quartz substrate using Van der Waals bonding, and finally patterned into a small area to be used in the CPS as a test-signal generator. As a simple preliminary example of the usefulness of such a structure, the vastly improved propagation characteristics of a CPS-on-quartz for millimeter-wave signals have been demonstrated, and the *S*-parameters of a capacitive gap in a coplanar stripline have been measured over a 300-GHz bandwidth. It is expected that these low-loss, low-dispersion transmission lines may also be incorporated as test fixtures in order to perform network analysis on active devices to very high frequency.

STRUCTURE PREPARATION

Fabrication

The LT-GaAs sample used in the lift-off procedure was grown by MBE at a substrate temperature of 190°C with post-annealing at MIT-Lincoln Laboratory. The top layer was 1 μm of LT-GaAs, grown on a thin $Al_{0.7}Ga_{0.3}As$ intermediate etch-stop layer on a semi-insulating GaAs substrate. The wafer was first coated with wax as described in ref. 4. After this step, the SI-GaAs substrate and $Al_{0.7}Ga_{0.3}As$ layers were subsequently removed by chemical etching (NH_4OH & H_2O_2 1:24 for SI-GaAs, Aqueous HF for $Al_{0.7}Ga_{0.3}As$). The remaining LT-GaAs film, supported by the wax, was placed onto a quartz substrate and held there with several tiny droplets of DI water. At this time, the surface tension of water pulled the LT-GaAs film and quartz substrate together. It was then found that baking was a very fast and effective way

CH3277-1/93/0000-1355$01.00 © 1993 IEEE

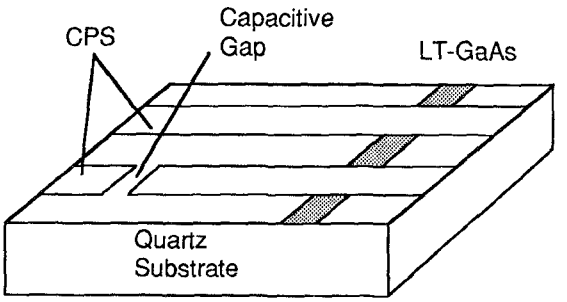

Figure 1: Simple test fixture for a gap capacitor. The LT-GaAs strip is bonded onto the quartz substrate by the Van der Waals force.

of forming the permanent bond between the two different materials, due to the atmospheric pressure which squeezed the air pockets left by the film of water after its molecules diffused out. The LT-GaAs film and the quartz substrate were thus pushed tightly together without the application of pressure on the wax as suggested in ref. 4. After the bond between these two materials was formed, the wax was rinsed away and standard processing steps were then used to form the structure shown in Figure 1. The Van Der Waals force bond, while offering only moderately strong adhesion between the LT-GaAs film and quartz substrate, was nonetheless found to be quite satisfactory during the subsequent patterning of deposited metalizations.

Quality of the LT-GaAs thin film on quartz

The main concern with the Van Der Waals bonding process was in maintaining a high quality of the lift-off LT-GaAs thin film. Before and after the lift-off, the behavior of the material was evaluated in terms of its surface defects, carrier life time, and carrier mobility. The surface quality was determined by simple visual examination of the LT-GaAs on quartz under a microscope. No visible cracking was observed after the grafting of our LT-GaAs film using our process, and the only visible defects were a few dome-shaped bubbles resulting from trapped particles between the LT-GaAs film and the quartz substrate during processing.

To compare the carrier life time of samples before and after lift-off and grafting, a pump-probe transient reflectivity experiment [6] was implemented. The FWHM of the impulse response to an optical excitation of ~ 100-fs duration was found to be 320 fs for both the original and grafted LT-GaAs cases. Finally, the comparison of carrier mobility was performed by comparing the switching efficiency (ratio of the generated pulse amplitude to the dc bias in a photoconductive detector) of photoconductive elements fabricated from the grafted and non-grafted materials. The switching efficiency was also measured to be essentially the same, approximately 1.2% for 2.8 mW average laser power, for both the materials before and after grafting. Therefore, there is no increase in defects or degradation of carrier lifetime or mobility for the films of LT-GaAs that were removed from their substrates and bonded to new hosts.

High frequency dielectric property of quartz

Since the CPS must possess low relative loss characteristics over a frequency range of several hundred gigahertz, it was also necessary to verify that the dielectric properties of quartz were favorable in this frequency range. To that end, the complex permittivity of the quartz substrate was measured via coherent time-domain spectroscopy [7] to determine its complex dielectric function and to screen for any resonances in the loss tangent. The results indicated that $\varepsilon_r \approx 3.9$ between 300 GHz and 1 THz, with negligible loss. Therefore, quartz was proven to be a very useful material for our waveguide structure due to its low permittivity and low loss.

THEORY

Attenuation

With negligible substrate attenuation through the dielectric loss tangent, the primary losses for the CPS are ohmic resistive losses from the skin effect in the conductors and the effect of radiation. For conductive losses, the functional relation can be written as

$$\alpha_{cond} \propto \sqrt{\frac{f}{\sigma}}\frac{1}{2w}$$

where w is the metal line width, σ is the metal conductivity and f is frequency.

For radiation, an expression for attenuation is given as [8]

$$\alpha_{rad} = \pi^5 \frac{3-\sqrt{8}}{2}\sqrt{\frac{\varepsilon_{eff}(f)}{\varepsilon_r}}\left(1-\frac{\varepsilon_{eff}(f)}{\varepsilon_r}\right)^2 \frac{(s+2w)^2\varepsilon_r^{3/2}}{c^3 K'(k)K(k)} f^3$$

where s is the separation between the metal line, ε_r is the substrate dielectric constant and ε_{eff} is the effective dielectric constant. The origin of the effective dielectric constant arises from the fact that the higher frequency components of the electric field in the propagating pulses tend to be confined more within the dielectric substrate, thus leading to a higher permittivity in this regime. In order to get a simple functional relation, $\varepsilon_{eff}(f)$ is set to the low-frequency limit, or $\varepsilon_{eff}(f)=(\varepsilon_r+1)/2$. After simplifying the above radiation loss equation, the functional relation can be expressed as

$$\alpha_{rad} \propto \frac{(\varepsilon_r+1)^{1/2}(\varepsilon_r-1)^2}{\varepsilon_r}(s+2w)^2 f^3$$

By substituting the permittivities for GaAs (ε_r ~12) and quartz (ε_r = 3.85) into the above equation, it was found that the radiation loss for the CPS on quartz was only 11% of that for the CPS on the GaAs substrate. Thus, one may conclude that reducing the substrate permittivity is a better way to decrease the radiation loss in a coplanar line, as compared to reducing the width of the metal line, since this would also serve to enhance the ohmic losses.

Dispersion

The well-known expression for the cutoff frequency of the first surface wave for microstrip line has been used to determine a figure of merit in order to compare the degree of dispersion for a CPS on either GaAs or quartz. From the expression,

$$f_{te} = \frac{c}{4h\sqrt{\varepsilon_r - 1}}$$

one can see that essentially the dispersion increases with the square root of the permittivity of the substrate. It is thus found that the cutoff frequency for the CPS on quartz would be approximately twice as great as that on GaAs, giving the quartz

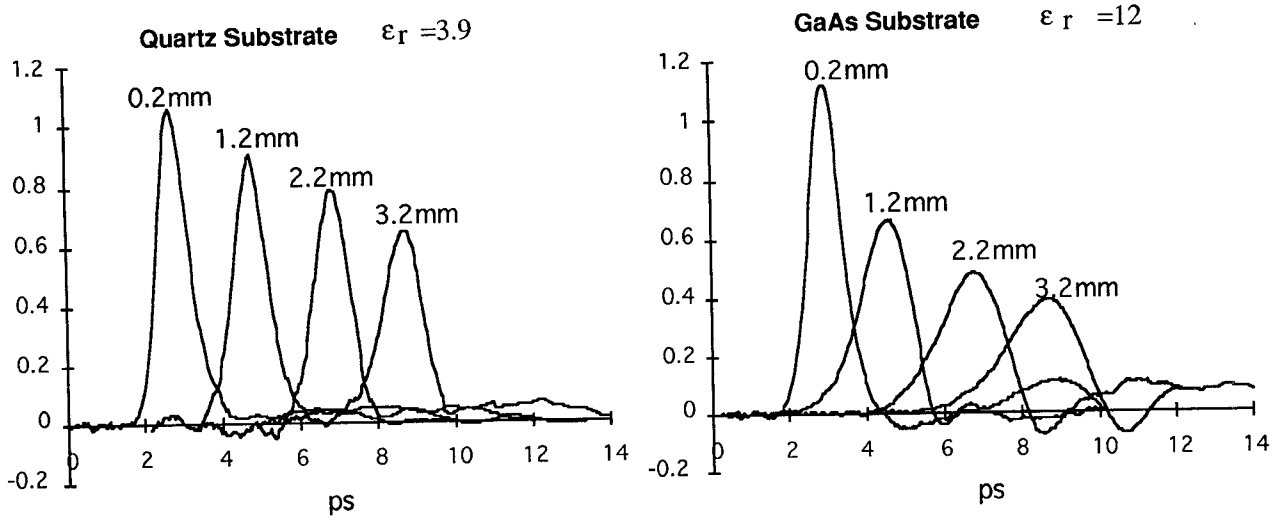

Figure 2: Time Domain pulse propagation data for CPS on GaAs and quartz substrates. The CPS-on-quartz has significantly lower attenuation and dispersion.

line a substantially smaller dispersion effect for the frequencies of interest.

MEASUREMENT

A balanced colliding pulse mode-locked dye laser with 80-fs pulse duration was used in the generation and detection of the electric signals on the transmission line integrated with the photoconductive switch. When the dc-biased CPS was temporarily shorted by the laser-excited carriers in the LT-GaAs film, a subpicosecond electric pulse was generated due to the short carrier life time (320 fs) of the LT-GaAs. The propagation of this pulse on the CPS was then measured by external electro-optic sampling [9], which uses a small probe tip of $LiTaO_3$ as a non-electrical-contacting transducer. This probe transformed the time-varying electric-field on the CPS into an amplitude modulation of the short laser pulses, and it was used to measure the necessary electrical signals propagating on the CPS lines with subpicosecond temporal resolution.

Figure 2 shows the measured time-domain waveforms from 0.2-mm to 3.2-mm propagation distances with 1-mm steps for signals on the quartz and GaAs transmission lines. This figure demonstrates the vast improvement obtained from the use of the low-permittivity substrate. The electrical pulse propagation on the CPS-on-quartz shows a significantly smaller attenuation and dispersion than that on the GaAs substrate. For instance, after 3.2 mm of propagation, the pulse on the GaAs line already has spread to 2.1 ps FWHM, while in contrast, the pulse on the quartz line only is only 1.18 ps FWHM. Furthermore, the amplitude of the pulse on the quartz line is over 60% of its original amplitude, while the signal on the GaAs line has degraded to less than 40% of its original voltage. The modal dispersion is also much more in evidence for the CPS-on-GaAs, as noted by the enhanced ringing in the tails of the signals.

RESULTS

Through numerical Fourier transformation of the time-domain data in Fig. 2, the attenuation and the effective permittivity in the frequency domain were calculated for the CPS lines on quartz and GaAs. Since the external electro-optic sampling measurements were very sensitive to the position of the probe with respect to the CPS under test, there are 10% to 15% variations between the measurements of different waveforms. To overcome this problem, a number of data sets were taken for each propagation distance and then averaged to reduce the error. Figure 3a shows the attenuation for the CPS on both GaAs and quartz. Clearly, the CPS on quartz has substantially smaller attenuation, particularly at the higher frequencies where the radiation loss dominates. Figure 3b shows the effective permittivity versus frequency for the lines measured, indicating that the dispersion of the quartz line was also much smaller than the GaAs line. Figure 4 displays an additional quantification of the bandwidth changes during the course of the waveform propagation. Because the frequency components over 200 GHz will radiate into the substrate very quickly for the CPS on GaAs, there is a large reduction in both the bandwidth and amplitude over the first 1 mm of propagation (see also Fig. 2). After these high-frequency components have radiated away, the dominant loss then becomes the skin effect loss which manifests itself as a linear drop in the bandwidth. However, for the CPS on quartz, the loss is dominated by the skin effect loss right from the beginning, so the bandwidth of CPS on quartz is not limited by the radiation loss for frequencies up to several hundred gigahertz.

Due to its much smaller attenuation and dispersion, the test fixture with the LT-GaAs grafted on the quartz substrate has a considerably larger characterization bandwidth, allowing the acquisition of more accurate amplitude and phase information for *S*-parameter measurements. As an example of the potential network analysis application of this time-domain technique, reflection and/or transmission measurements were made on several simple passive circuit elements, such as the gap capacitor in Fig. 1 and an open ended CPS. In each case, distinct incident and reflected (and when applicable, transmitted) waveforms from the components under test were acquired in the time domain and then processed to obtain the requisite spectral information. While the temporal signals are not shown here, clearly defined time windows, free from deleterious reflections and superpositions, were identified.

Figure 5 shows a polar plot of the S_{11} and S_{21} for a 10-μm-long, in-line capacitive gap for frequencies between 50 and 300 GHz. This basically illustrates the reduction of the impedance of the capacitor with increasing frequency. The capacitance of the

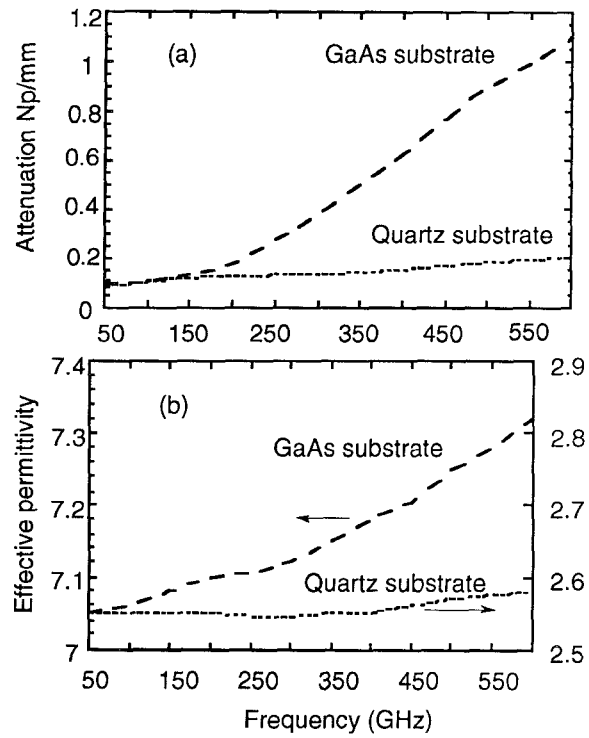

Figure 3: Frequency domain attenuation (a) and permittivity (b) data for CPS on GaAs and on quartz substrate. The CPS on quartz can support a much wider bandwidth.

gap was determined to be 78 fF by fitting the S-parameter curve with a simple high-frequency circuit model. As there are some deviations at high frequency which suggest that the gap can not simply be represented as a capacitor, a modification of this model is needed.

CONCLUSION

To conclude, the grafted-LT-GaAs-on-quartz test fixture has proven to be very effective in a high-frequency passive device measurement. Optoelectronics, especially laser-based diagnostics that will be able to take advantage of the rapid development in compact semiconductor and solid-state high-speed lasers, should provide outstanding opportunities for the high-frequency characterization of microelectronics. It is also believed that the epitaxial lift-off technology can be extended to the grafting of an active device to the quartz substrate utilized in this investigation, leading to a high-speed and low-distortion device interconnection. Furthermore, by applying the standard device passivation layer (SiO_2) to the integrated devices and test fixtures used here, there will automatically be formed a superstrate on the quartz circuit with a similar permittivity to this substrate. Therefore, further improvements in the interconnection performance are expected as more effort is expended toward the goal of higher frequency characterization.

Acknowledgement: This research is supported by AFOSR contract number AFOSR-90-0214 (University Research Initiative) and by the National Science Foundation through the Center for Ultrafast Optical Science under STC PHY 8920108.

REFERENCES

[1] M.Y. Frankel *et al., IEEE Trans. Microwave Theory Tech.*, vol. 39, p.910 (1991).
[2] M.Matloubian, et al., *IEEE Trans. Microwave Theory Tech.*, vol. 38, p.682 (1990).
[3]C.H.Lee, *IEEE Trans. Microwave Theory Tech.*,vol.38,p.596 (1990).
[4] E. Yablonovitch *et al., Appl. Phys. Lett.*, vol 56, p.2419 (1990).
[5] F.W. Smith *et al., Appl. Phys. Lett.*, vol 54, p.890 (1989).
[6] M.Y. Frankel *et al., OSA Proceedings on Picosecond Electronics and Optoelectronics*, T.C.L.G. Sollner, J. Shah, eds., (Optical Society of America, Washington, DC 1991), vol. 9, pp. 146-150.
[7] J. Chwalek *et al., Electronics Lett.*, vol. 27, Feb. 1991, pp. 447-448.
[8] M.Y. Frankel *et al., IEEE Trans. Microwave Theory Tech.*, vol. 39, June 1991, pp.910-916.
[9] J.A. Valdmanis *et al., IEEE J. Quantum Electronic.*, vol. QE-22, p.69 (1986)

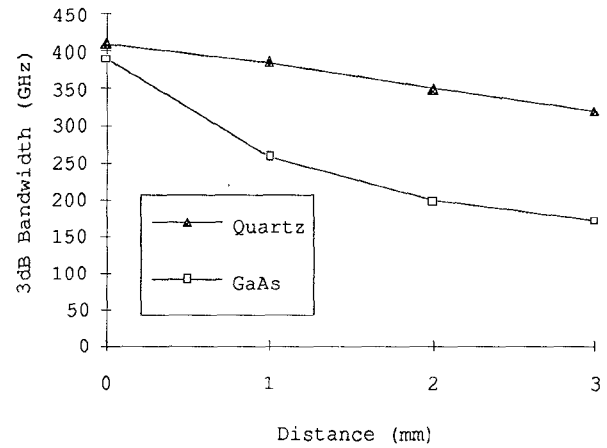

Figure 4: Pulse bandwidth (top) and amplitude (bottom) vs. propagation distance

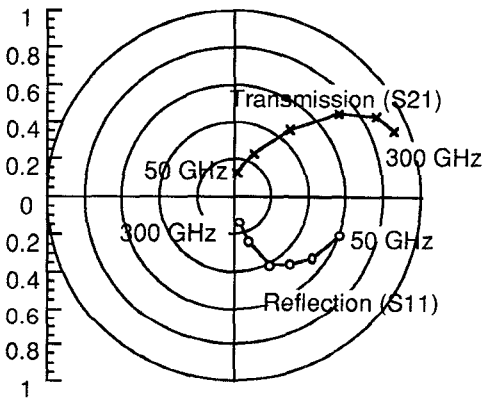

Figure 5: S-parameters for a gap capacitor to 300 GHz.